RESEARCH PAPER

MHD mixed convection flow of alumina - water nanofluid into a lid-driven cavity with different patterns of wavy sidewalls

Ahmed Kadhim Hussein [1], Watit Pakdee [2, *], Mohamed Bechir Ben Hamida [3,4,5], Bagh Ali [6], Farhan Lafta Rashid [7], Uddhaba Biswal [8] and Muataz S .Alhassan [9]

[1] College of Engineering -Mechanical Engineering Department -University of Babylon - Babylon City, Hilla, Iraq
[2] Center for R&D on Energy Efficiency in Thermo-Fluid Systems, Department of Mechanical Engineering, Thammasat University, Klong Nueng, Klong Lueng, Pathum Thani, Thailand
[3] College of Engineering, Department of Chemical Engineering, Imam Mohammad Ibn Saud Islamic University (IMSIU), Riyadh, Saudi Arabia
[4] Research Laboratory of Ionized Backgrounds and Reagents Studies (EMIR), Preparatory Institute for Engineering Studies of Monastir (IPEIM), University of Monastir, Monastir City, Tunisia.
[5] Higher School of Sciences and Technology of Hammam Sousse (ESSTHS), Department of Physics, University of Sousse, Sousse City, Tunisia.
[6] School of Mechanical Engineering and Automation, Harbin Institute of Technology, Shenzhen 518055, China
[7] Petroleum Engineering Department, College of Engineering, University of Kerbala, Kerbala, Iraq
[8] Department of Mathematics, Laxminarayan College, Jharsuguda, Odisha 768202, India
[9] Division of advanced nano material technologies, Scientific Research Center, Al-Ayen University, Thi-Qar, Iraq

Abstract

This research investigates the numerical analysis of magnetohydrodynamic (MHD) mixed convection flow and heat transfer within a bottom lid-driven cavity filled with water-alumina (Al2O3) nanofluid. The cavity's sidewalls exhibit a wavy profile and are maintained at distinct temperatures. Cavity domain exhibit distinct free and force convections. These wavy walls, characterized by zigzag shapes determined by various wave amplitudes and their ratios (wave form), create a dynamic thermal environment. The top and bottom surfaces remain flat and well-insulated, while forced convection is induced by the drag of the bottom wall from left to right at a constant speed. Additionally, the bottom wall is subjected to a vertical magnetic field. The system of equations is discretized using the finite difference method. The numerical solutions are derived by the Gauss-Seidel iterative method. The study primarily focuses on investigating the effects of key parameters, including the wavy wall geometry, solid volume fraction ($0 \leq \varphi \leq 0.0003$), Rayleigh number ($10^3 \leq Ra \leq 10^5$), and Hartmann number ($0 \leq Ha \leq 0.6$). Numerical solutions are computed across different ranges of these parameters, and the obtained results are successfully validated against previous numerical studies. The findings reveal that higher Hartmann numbers and solid volume fractions lead to lower circulation rates and Nusselt numbers. Convection is markedly enhanced with higher amplitude and its ratios of the wavy sidewalls. The combined two-sinusoidal function with the wave amplitudes of 2.5 and 0.47 of provides the highest mean Nusselt

* Corresponding author. *E-mail address:* pwatit@engr.tu.ac.th

numberof3.204 with the highest dimensionless stream function of 1.638. These results highlight the significant influence of the wave form on both flow and temperature distributions.

Keywords: Nanofluid; Mixedconvection; Magnetic effect; Wavycavity; Lid-driven; Wavy pattern; Wave form

Nomenclature

B_o	magnitude of the magnetic field, Tesla
c_p	specific heat at constant pressure, j / kg. °C
g	gravitational acceleration, m/s^2
H	height of the cavity, M
Ha	Hartmann number
k	thermal conductivity, W / m. °C
l_w	length of wavy surface, M
Nu	Nusselt number
N	normal direction
p	pressure, N/ m^2
Pr	Prandtl number
Ra	Rayleigh number
R_α	Amplitude ratio of wavy surface
T	temperature, °C
U	lid-driven velocity, m/s
u	velocity component in x-direction, m/s
v	velocity component in y-direction, m/s
W	width of the cavity, m
x	cartesian coordinate in horizontal direction, m
y	cartesian coordinate in vertical direction, m

Greek Symbols

α	thermal diffusivity, m^2/s
α_1, α_2	amplitude of wavy surface
β	coefficient of thermal expansion, K^{-1}
θ	dimensionless temperature
σ	electrical conductivity, W / m. °C
φ	solid volume fraction
ν	kinematic viscosity of the fluid, m^2/s
μ	viscosity of the fluid, kg /m.s
ρ	density, kg/m^3
η	parameter to avoid the zero dominator
λ	wave length of wave surface

Subscripts

c	cold
f	fluid particle
h	hot
nf	nano fluid property
m	mean or average
p	solid particle
w	wall

Superscripts

∗	dimensionless

1. Introduction

Nanofluids were introduced as a promising technique to enhance heat transfer. Highly thermal conductive nanoparticles are incorporated to industrial fluids including water, refrigerants, ethylene glycol, kerosene, acetone and engine lubricant, to boost their various thermal properties. These new kinds of fluids are manufactured by the dispersion of nanoparticles in regular fluids. In engineering applications such as energy storage, automotive coolant, electronic cooling systems, nuclear devices, conversion system of solar energy, and pharmaceutical procedures, due to its superior thermal performance, nanofluids have become essential. Subsequently, a notable amount of study on nanofluids spread to various domains like the determination of their thermophysical properties, their influence on flow behavior, heat transfer characteristics, etc.[1].

Accordingly, mixed convection within classical cavities filled with nanofluids, including the case of lid-driven walls, is worth investigation. Muthtamilselvan et al.[2] numerically examined the mixed convection for different aspect ratios in a lid-driven enclosure filled with copper-water nanofluids and reported that the fluid flow and heat transfer in the lid-driven cavity were influenced by both aspect ratio and solid volume fraction. Moreover, the solid volume fraction could have a beneficial impact on heat transfer enhancement at specific values of Reynolds and Rayleigh numbers [3]. Shahi et al.[4] also conducted a numerical simulation of mixed convection fluxes of copper-water nanofluid through a square duct with inflow and outflow ports and found that the higher solid content resulted in the higher average Nusselt number at the heated surface and the lower bulk temperature. Salari etal. [5] investigated mixed convection flow inside a square lid-driven cavity filled with different nanofluids where the bottom and side surfaces of were simultaneously heated.Furthermore, under the same conditions, the Nusselt number exhibited larger values when utilizing alumina (Al_2O_3) nanoparticles, whereas the addition of titanium dioxide (TiO_2) nanoparticles resulted in smaller Nusselt numbers. This discrepancy could be attributed to the differing thermophysical properties of the nanoparticles. Nasrin et al. [6] analyzed the mixed convection of water-CuO nanofluid in a two-sided lid-driven cavity in which heat was internally generated. They found that the Richardson number significantly influenced the heat transfer characteristics within the triangular container. Additionally, the numerical results indicated that the flow behavior clearly changed with the volume fraction of nanoparticles. Over the past decade, Buongiorno's model has been applied in the studies of heat transport in nanofluids to describe heat flows which are caused by Brownian motion and thermophoresis effect [7, 8]. In the problem of mixed convective heat transfer in a lid-driven cavity filled with a water-based nanofluid, a dependence of heat and mass transfer mechanisms on the Richardson number and moving parameter was found to be significant [7].

At low Reynolds numbers, the increment of Al_2O_3 nanoparticles caused a negative effect on the heat convection for very high values of Richardson number [8].

The investigation of mixed convection heat transfers in enclosures with wavy walls involving nanofluids is a subject of considerable interest in various industrial applications, including cooling systems for microelectronic devices, electronic packages, solar collectors, heat exchangers, and many more [9, 10].Cavities often clearly exhibit natural convection, where heat transfer occurs due to fluid movement driven by temperature differences. Effects of natural convection relative to force convection can be fundamentally investigated. Cavities are used as simplified models to explore complex phenomena, helping to develop theories and models that can be applied in more general contexts. The inclusion of wavy walls in these enclosures offers a notable advantage compared to flat walls, as they contribute to heightened efficiency in heat exchange with the surroundings. This is primarily attributed to the expanded surface area of the walls within the identical cavity size, facilitating improved heat transfer capabilities [9]. In a similar vein, Jafari et al. [10] employed the Lattice Boltzmann Method (LBM) to examine how the properties of a wavy wall affected the mixed convection of water-Al2O3 nanofluid in a lid-driven cavity. The findings indicated that the addition of nanoparticles to the base fluid had important impacts on both the flow pattern and temperature distribution during mixed convection, particularly at low Richardson numbers. In a similar vein, Cho et al. [11] performed a numerical investigation of mixed convection in a lid-driven cavity with wavy walls filled with different nanofluids, including Cu-water, Al2O3-water, and TiO2-water. The researchers concluded that the heat transfer rate was higher for copper nanoparticles compared to other types of nanoparticles. Wavy amplitude and the number of undulations of wavy walls significantly influenced both Nusselt number and entropy generation [12-14]. Continuing the research, Buongiorno's two-phase model was utilized to investigate transient mixed convection in a nanofluid-filled cavity with wavy walls, where both vertical walls were lid-driven, and there was an internal circular heat conducting block at the center [15]. The wavy form of the wall combined with the characteristics of nanofluid and interior cylinder found to be the important controlling parameter for heat transfer rate and flow process. By using the headline visualization technique, Azizul et al. [16] investigated numerically the mixed convection flow in a heated cavity with waves that was filled

with nanofluids and had an inner solid block.It was concluded that a smaller curved surface with both sides of a crumpled wavy lid-driven cavity could be identified as an effective heat transfer mechanism. Recently, optimization studies were conducted to obtain optimal associated parameters for heat transfer in a wavy enclosure [17-19]. Based on the ideal thermal design, the optimal Nusselt number was achieved by using response surface method (RSM) and Taguchi method [19].

Apart from the intricate geometries used to simulate engineering applications, the magnetic field has emerged as a valuable option that contributes to improving heat transfer within cavities, particularly when combined with the use of nanoparticles. The influence of magnetic fields on heat transfer and fluid flow has gained significant attention in recent years due to its relevance in various areas, including micro-electronic devices, purification of molten metals, cooling devices for nuclear reactors, MHD power generation, and more [20]. A large number of studies have been conducted to investigate the utilization of an external magnetic field for controlling heat transfer and fluid flow characteristics. Öztop et al. [21] studied the laminar mixed convection flow in a lid-driven enclosure with heating at the corner, considering the influence of magnetic force. They concluded that the magnetic field significantly affects the control of heat and fluid flow, while the dimensions of the heater play a crucial role in the dominant regime of natural convection.Selimefendigil and Öztop [22] examined MHD mixed convection in a square enclosure filled with a nanofluid and driven by a lid, which also included a rotating cylinder. Their findings indicated that the magnetic field can be utilized to control heat transfer by enhancing it towards the right end of the bottom wall.In the study by Hussain et al. [23], the mixed convection of Al2O3-water nanofluid was explored in a square double lid-driven cavity with an inclined magnetic field, discrete heating, and entropy generation. These studies highlight the significant impact of utilizing external magnetic fields in controlling heat transfer and fluid flow characteristics in various cavity configurations and nanofluid systems.

The effects of a changing magnetic field on mixed convection in a lid-driven enclosure with a sinusoidal hot surface were examined by Sheikholeslami and Chamkha [24]. According to their research, increasing the magnetic number, nanoparticle volume percent, and Reynolds number increases the rate of heat transfer, however the Hartmann number had the opposite effect. Öztop et al. [25] studied the effects of magnetic field on the mixed convection fluid flow within a wavy walled cavity having a lid-driven wall and filled with CuO-water nanofluid. Although, in this work, the wavy wall was simply a single-bulged bottom wall, heat transfer is strongly influenced by the nanoparticles volume fraction according to Hartmann and Richardson numbers.Mixed convective heat transfer in a lid-driven cavity considering the effects of volumetric heat generation or consumption was carried out to examine the impact of an inclined magnetic field [26]. In a separate study, Alsabery et al. [27] employed the two-phase nanofluids method using alumina nanoparticles to numerically investigate transient mixed convection in a lid-driven wavy chamber containing a solid cylinder subjected to a uniform magnetic field. The findings revealed that an increase in the number of undulations reduced energy transport, while selecting an appropriate internal cylinder radius intensified heat transfer. A recent study utilized carbonnanotudes (CNT) in nanofluid to investigate the magnetohydrodynamic (MHD) mixed convection of CNT-waternanofluid in a wavy porous enclosure [28]. Furthermore, thermal analysis and optimization study were carried out for heat transfer in hybrid nanofluids subjected to magnetic field in porous cavities [29-31] The Rayleigh number had the most colossal contribution comparing other factors on the achieved optimal value of the involved parameters in an octagonal cavity [31].Top of Form

In the context of the literature review presented in this paper, considerable efforts have been made by researchers to enhance heat transfer within enclosures. These endeavors encompass not only the exploration of nanofluids but also various modifications to the geometry of the enclosures. It is apparent that these techniques hold the potential to improve heat transfer performance within enclosures [32, 33].Adjusting the wavy surface geometry parameters could potentially increase the mean Nusselt number for a specific nanofluid [11]. However, the intricate interplay of magnetic fields, nanomaterials, nanofluid volume fraction, and wavy geometry remains not fully comprehended. Moreover, although irregular cavities with corrugated or wavy walls are presently utilized, they have received comparatively less attention in the literature when contrasted with traditional geometries. This lack of attention is attributed to the challenges associated with defining enclosure boundaries, directly influencing the flow within such enclosures. Consequently, the present study delves into the combined effects on the magneto-hydrodynamics (MHD) mixed convection behaviors of nanofluid in a cavity with specifically defined wavy sidewalls. Different waveforms dictate the waviness of the enclosure side walls. The nanoparticle considered in this study is Al2O3 due to its excellent thermal performance [34, 35]. The quantitative outcomes provide a comprehensive understanding of how the Rayleigh number, solid volume fractions, wavy-surface geometry parameters, and Hartmann number collectively impact mixed convection involving magneto-hydrodynamics in a water-Al_2O_3 nanofluid-filled, lid-driven wavy cavity. This complex problem incorporates various interrelated effects, including wall shape geometry. To the best of the authors'

knowledge, a comprehensive investigation considering all these combined effects has not been reported in the literature.

2. Problem Formulation

Schematic representation of a two-dimensional wavy lid-driven cavity of height (H) and width (W) is shown in Fig 1. The left and right sidewalls have a zigzag-shaped surface and are maintained at different specified temperatures. The top and bottom walls are straight and perfectly insulated. The cavity contains a nanofluid consisting of water-Al2O3. A uniform magnetic field with a magnitude (Bo) is applied vertically downward onto the cavity. Meanwhile, the bottom wall is assumed to move from left to right at a constant lid-driven velocity (U). The gravitational force acts in the negative y-direction. The range of the Hartmann number is [0 ≤Ha ≤0.6], and the range of the Rayleigh number is [103≤ Ra ≤105], encompassing both buoyancy and magnetic field dominant flow regimes. The Prandtl number is fixed at Pr = 6.2. The solid volume fractions (φ) are varied within [0 ≤ φ ≤0.0003]. Table 1 lists the base fluid's and nanoparticles' thermo-physical properties [36]. The governing equations are developed based on the following assumptions [37]:

1. The flow field is steady and laminar.
2. While the Boussinesq approximation is considered to model density variation, the thermo-physical characteristics of base fluid (water) and nanoparticles are assumed to remain constant.
3. The nanoparticles are evenly distributed throughout the base fluid and are of a homogeneous size and shape.
4.   The base fluid and the nanoparticles are in a condition of thermal equilibrium with no slip between the two phases.
5. The viscous dissipation is negligibly small.
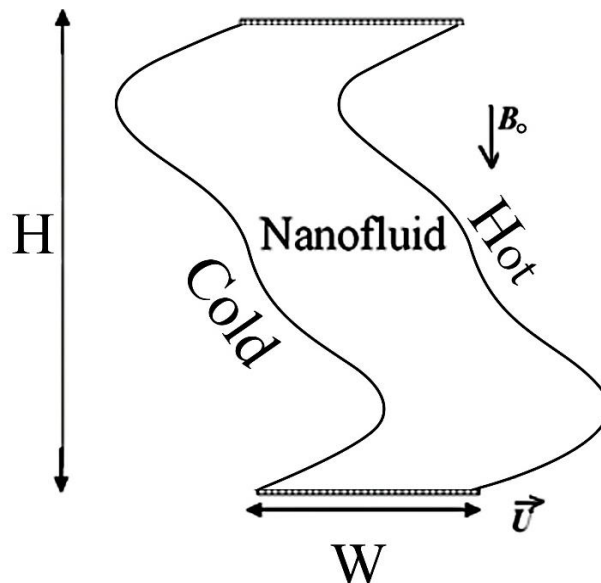
Fig 1: Physical model of the problem.

Table 1: Thermo physical properties [36]

Properties	Water	Al₂O₃
C_p	4179	756
k	0.613	40
α	1.47×10^{-7}	131.7×10^{-7}
β	21×10^{-7}	0.85×10^{-5}
ρ	997.1	3970

3. Governing equations

Based on the appropriate assumptions, the set of equations governing the specified problem include continuity, momentum and energy transport equations [23].

$$\frac{\partial u}{\partial x} + \frac{\partial u}{\partial y} = 0 \tag{1}$$

$$u\frac{\partial u}{\partial x} + v\frac{\partial u}{\partial y} = -\frac{1}{\rho_{nf}}\frac{\partial p}{\partial x} + \frac{\mu_{nf}}{\rho_{nf}}\nabla^2 u - \frac{\sigma_{nf}}{\rho_{nf}}B_0^2 u \tag{2}$$

$$u\frac{\partial v}{\partial x} + v\frac{\partial v}{\partial y} = -\frac{1}{\rho_{nf}}\frac{\partial p}{\partial x} + \frac{\mu_{nf}}{\rho_{nf}}\nabla^2 v - \frac{g}{\rho_{nf}}\left((\rho\beta)_f(1-\varphi) + (\rho\beta)_s\varphi\right)(T - T_c) \tag{3}$$

$$u\frac{\partial T}{\partial x} + v\frac{\partial T}{\partial y} = \propto_{nf}\nabla^2 T \tag{4}$$

The system of equations undergoes a non-dimensionlization process to simplify and scale equations by removing the inherent physical units by using following dimensionless parameters.

$$x^* = \frac{x}{W}, y^* = \frac{y}{W}, u^* = \frac{u}{U}, v^* = \frac{v}{U}, p^* = \frac{p}{\rho_f \alpha_f^2 / W^2}$$

$$\theta = \frac{T - T_c}{T_h - T_c} \tag{5}$$

The non-dimensionalized equations for the steady state magneto-hydrodynamic flow are given by [after dropping the super script*]: -

$$\frac{\partial u}{\partial x} + \frac{\partial v}{\partial y} = 0 \tag{6}$$

$$u\frac{\partial u}{\partial x} + v\frac{\partial u}{\partial y} = -\frac{\partial p}{\partial x} + \frac{\mu_{nf}}{\rho_{nf}\alpha_f}\nabla^2 u - Ha^2 Pr\frac{\sigma_{nf}}{\sigma_f}\frac{\rho_f}{\rho_{nf}}u \tag{7}$$

$$u\frac{\partial v}{\partial x} + v\frac{\partial v}{\partial y} = -\frac{\partial p}{\partial y} + \upsilon_{nf}\nabla^2 v + PrRa\frac{\rho_f}{\rho_{nf}}\left((1-\phi) + \phi\frac{(\rho\beta)_s}{(\rho\beta)_f}\right)\theta \tag{8}$$

$$u\frac{\partial \theta}{\partial x} + v\frac{\partial \theta}{\partial y} = \alpha_{nf}\nabla^2\theta \tag{9}$$

The dimensionless groups or parameters resulted from the non-dimensionalization are:

$$Pr = \left(\frac{\nu}{\alpha}\right)_f, Ra = \frac{g\beta_f[T_h - T_c]W^3}{(\nu\alpha)_f}, Ha = B_o W\sqrt{\frac{\sigma_f}{\rho_f \upsilon_f}} \tag{10}$$

These dimensionless groups or parameters provide insights into the relative importance of different physical effects and are valuable for making comparisons across different scales or systems.

The nanofluid thermal diffusivity, density, heat capacitance and the dynamic viscosity are given by the following equations respectively [37]:

$$\alpha_{nf} = \frac{k_{nf}}{(\rho c_p)_{nf}}$$ (11)

$$\rho_{nf} = (1 - \varphi)\rho_f + \varphi\rho_p$$ (12)

$$(\rho c_p)_{nf} = (1 - \varphi)(\rho c_p)_f + \varphi(\rho c_p)_p$$ (13)

The effective viscosity of nanofluid is approximated by the Brinkmann model [38]

$$\mu_{nf} = \frac{\mu_f}{(1 - \varphi)^{2.5}}$$ (14)

While, the effective thermal conductivity of the nanofluid is determined to be a function of solid volume fraction and the base fluid properties as [13]:

$$\frac{k_{nf}}{k_f} = \frac{(k_p + 2k_f) - 2\varphi(k_f - k_p)}{(k_p + 2k_f) + \varphi(k_f - k_p)}$$ (15)

3.1. Local and average Nusselt numbers along the wavy wall surface

The local and average Nusselt numbers along the wavy wall surface can be written as-:

$$Nu = -\frac{k_{nf}}{k_{bf}}\left(\frac{\partial\theta}{\partial n}\right)_w$$ (16)

$$Nu_m = \frac{1}{l_w^*}\int_0^{l_w^*} Nu\,d\eta$$ (17)

where, l_w^* is the length of the hot wavy surface.

3.2. Wavy-wall configuration profile

The dimensionless profile of the considered wavy sidewalls which have a zigzag shape is modeled. It is described by the combined sinusoidal functions given by [39]:

$$x^* = \alpha_1 sin\left(\frac{2\pi y^*}{\lambda}\right) + \alpha_2 sin\left(\frac{4\pi y^*}{\lambda}\right)$$ (18)

where λ is the wavelength, and α_1 and α_2 are amplitudes of the two functions.
Three different cases of the zigzag surface are prescribed as follows: -
For case 1 $\alpha_1 = 0.5$ and $R_\alpha = 0.2$
For case 2 $\alpha_1 = 2.5$ and $R_\alpha = 0.188$
For case 3 $\alpha_1 = 0.607$ and $R_\alpha = 0$,
where R_α denotes the amplitude ratio of the two wave functions given as

$$R_\alpha = \frac{\alpha_2}{\alpha_1} \tag{19}$$

3.3. Boundary conditions

The left and the right wavy walls are kept at a constant cold (Tc), and hot (Th)temperatures, in order to replicate the flow and thermal fields in the zigzag wavy cavity. The adiabatic condition is imposed at the top and bottom walls. Finally, all of the cavity wall surfaces other than the bottom one are subjected to an impermeable no-slip condition. Following is a summary of the non-dimensional boundary conditions:

1. The bottom wall of the cavity is assumed adiabatic and moves from left to right with a uniform velocity,i.e.,

$$\text{at } y^* = 0 \quad \frac{\partial \theta}{\partial n^*} = 0, u^* = 1 \text{ and } v^* = 0 \tag{20}$$

2. Adiabatic condition is imposed at the top wall of the cavity,i.e.,

$$\text{at } y^* = 1 \quad \frac{\partial \theta}{\partial n^*} = 0, \quad = v^* = 0 \tag{21}$$

3. The left sidewall is prescribed as the cold side, i.e.,

$$\text{at } x^* = 0 \quad \theta = 0, u^* = v^* = 0 \tag{22}$$

4. The right sidewall is prescribed as the hot side, i.e.,

$$\text{at } x^* = 1 \quad \theta = 1, u^* = v^* = 0 \tag{23}$$

4. Numerical procedure and model validation

The governing equations and their respective boundary conditions are solved using the finite difference method, as outlined by Mansour et al. [40]. Central difference approximations are utilized to estimate the second derivatives of variables. The Gauss-Seidel iteration algorithmis applied to solve the resulting discretized equations for the dependent variables u*, v* and θ [41, 42]. The iteration progressively continues until the specified convergence criterion is met.:

$$max|\chi_{i,j}^{new} - \chi_{i,j}^{old}| \leq 10^{-7} \tag{24}$$

where χ is the computed values of u*, v* and θ. A FORTRAN software is utilized to implement the numerical computation. To find the optimum grid resolution, the grid independence test was carried out. The maximum stream function and mean Nusselt number were computed for$\varphi = 10^{-4}$, Ra= 10^5, and Ha=0.5 The finite difference approach employed five sets of grid resolutions, namely [26×26, 51×51, 76×76, 101×101, 121×121].The results are shown in Table 2. Comparing the (76×76), 101×101and (121×121) grids reveals a high level of agreement. Therefore, the present computations are performed using the (76×76) and (101×101) grid nodal points.CPU (8 cores, 16 threads) with 16 GB DDR4 RAM was utilized for computations. As for an example to get an idea for a CPU time taken, it took 183 seconds for $\varphi = 10^{-4}$, Ra = 10^5, and Ha = 0.5 with 101×101 resolution.

To assess the accuracy of the proposed method, the results were compared with the findings of Grosan et al. [41]and Haajizadeh et al. [43]under specific cases. In [41], the steady natural convection within the square porous cavity with internal heat generation were tested. The system of equations was discretized using a central finite-difference scheme, while the Gauss-Seidel iteration algorithm was used to solve for the numerical solutions [41]. For the other steady problem, buoyancy-induced flow due to internal heat generation was investigated [43]. Asymptotic solutions were solved by expanding stream function and temperature in power series. Table 3 demonstrates a satisfactory agreement between the present results and those obtained from the previous studies. These successful validation yield confidence in the subsequent reporting of the computed results.

<center>**Table 2: Results of grid independence study**</center>

Resolution	Ψ_{max}	Nu_m
26x26	1.605	3.176
51x51	1.633	3.198
76x76	1.637	3.203
101x101	1.638	3.204
201x201	1.638	3.204

<center>**Table 3: Validation of the numerical model**</center>

Ra	Haajizadeh et al. [43]		Grosan et al. [41]		Present	
	Ψ_{max}	θ_{max}	Ψ_{max}	θ_{max}	Ψ_{max}	θ_{max}
10	0.078	0.130	0.079	0.127	0.0799	0.1272
10^3	4.880	0.118	4.833	0.116	4.8266	0.117

5. Results and Discussion

The MHD mixed convection flow and heat transfer in a wavy lid-driven cavity filled with water-Al_2O_3 nanofluid has been numerically carried out. During the numerical analysis of the current work, the Prandtl number is taken to be fixed at 6.2. Rayleigh number ranges from 10^3 to 10^5, the Hartmann number ranges from 0 to 0.6 while the solid volume fraction range $[0 \leq \varphi \leq 0.0003]$. Also, three different cases of the wavy surface are considered in this work.

5.1. Effect of Rayleigh number

The computed data are post-processed and shown in Fig 2 for the streamlines (left) and isotherms (right) for various Rayleigh numbers at Ha = 0.5 and $\varphi = 10^{-4}$. The Rayleigh number is a dimensionless parameter that provides a measure of a relative importance of buoyancy forces to viscous forces within a fluid. It is often used to predict the transition from a quiescent state to convective motion as the temperature gradient changes. The flow field is found to be characterized by two upper and lower re-circulating counterclockwise vortices of high intensity are generated between the cold left and hot right wavy walls. The buoyancy-driven flows are created. For the top vortex, the hot lighter fluid that moves upward hit the top wall. Then its flow direction changes while the colder fluid follows thereby inducing the circulations. Similarly, in case of the bottom vortex, the hot fluid floating up hits the slanted side wall causing the flow direction to change whereas the fluid near the cold wall descends. The induced circulations enhance heat transfer rate. Locations of high gradients of streamlines are around the sharp curved profile of the side walls. These locations appear to be similar to the locations where the isotherm gradients are high. This finding confirms how the streamline pattern influences the isotherm pattern. For low Rayleigh number $[Ra = 10^3]$, the viscous force dominates the buoyancy force. There appears an induced flow near the bottom wall due to the lid motion, which effectively modifies the circulation pattern of the bottom vortex since intensities of circulations are weak. However, for the case of high Rayleigh number $[Ra = 10^5]$, the circulations inside the cavity get strong. The flow circulation is intense at the cavity center and low in the vicinity of sidewalls due to no-slip boundary conditions. The re-circulating counterclockwise vortices inside the wavy cavity are rather symmetrical. Also, it is noticed that the bottom vortex is lifted up vertically. These results are attributed to the dominant buoyancy effect that conceals the forced convection effect. Moreover, the re-circulating counterclockwise vortices become denser as compared to the case of low the Rayleigh number. With respect to the thermal field, although their thermal behaviors do not show a significant difference between different Rayleigh numbers, the overall gradient of the isotherms along the hot wall is slightly higher at the larger Raof 10^5, causing greater heat convection. Extended investigation of the effect of Ra will be discussed further in Fig.6.The isotherms are roughly symmetrical and parallel to both of the sidewalls, respectively, showing that pure conduction is the primary mode of heat transport inside the wavy chamber.

(a)   Ra = 10^3

(b)   Ra = 10^5
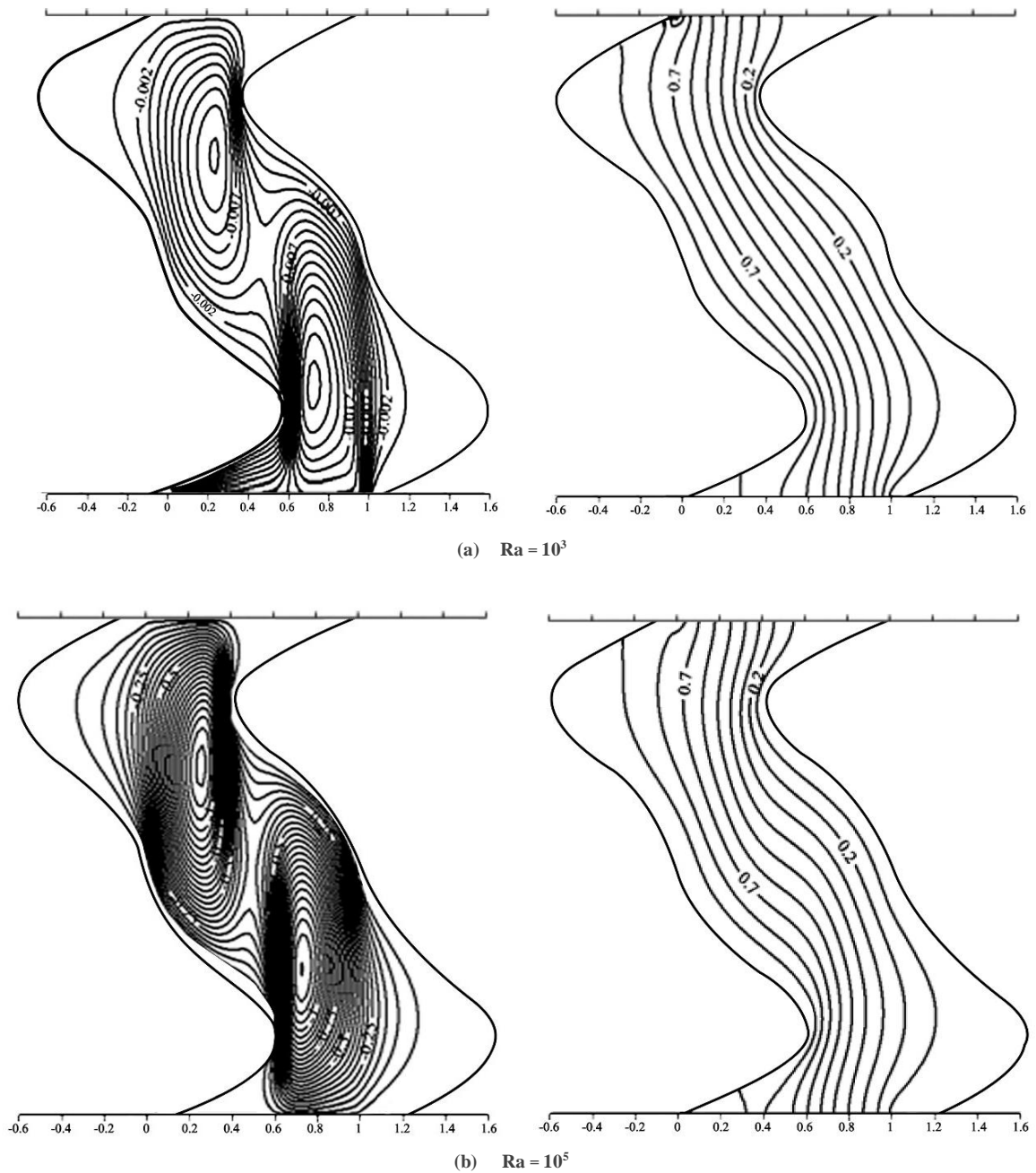
Fig 2: Streamlines (left) and isotherms (right) for various Rayleigh number at Ha = 0.5 and $\varphi = 10^{-4}$

5.2. Effect of Hartmann number

The Hartmann number is defined as the magnitude of the force induced by magnetic induction relative to the viscous force in the fluid flow. In Fig. 3(a) for small value of the Hartmann number (Ha = 0.2) corresponding to the weak magnetic field, the flow circulation is enhanced, as the buoyancy force essentially controls the flows. The streamlines are clustered adjacent the sidewalls. It is interesting that there appears the third circulation or vortex in between the two main vortices. This small clockwise-circulating vortex is generated by the two main vortices. In this case, the convection heat transfer becomes important while the magnetic effect is weak. On the other hand, when the Hartmann number increases (Ha = 0.5) as shown in Fig.3(b), the Lorentz force induced by magnetic field intensity becomes significant relative to the buoyancy force thereby weakening the flow circulation. As a consequence, the effect of convection is substantially diminished. Regarding the temperature contour, towards the low Hartmann

number (Ha = 0.2) corresponding to the weak magnetic field, the isotherms are concentrated highly inside wavy cavity and their shapes are curved according to directions of the three vortices. This result indicates that the mixed convection prevails. When the magnetic field is substantially strengthened at high Hartmann number (Ha = 0.5), the flows are suppressed by the magnetic force. The concentrated isotherms inside the wavy cavity become less compressed and isothermal lines turn to be straight and parallel adjacent to the sidewalls indicating that. the heat transfer inside the wavy cavity is mainly governed by heat conduction. Further analysis is carried out through the results given in Fig.7.

(a)   Ha = 0.2

(b)   Ha = 0.5
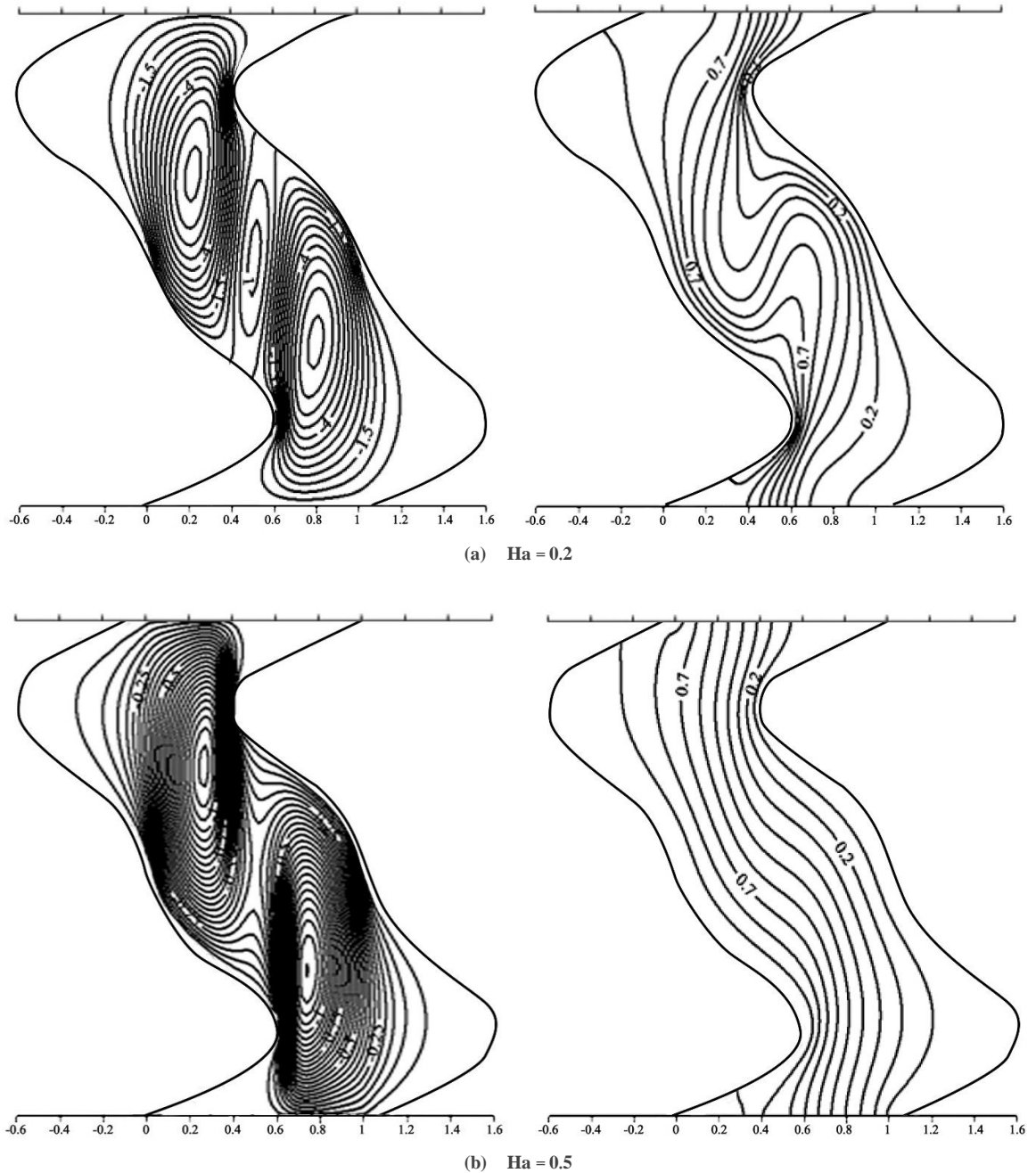
Fig 3: Streamlines (left) and isotherms (right) for various Hartmann number at Ra=10^5 and φ =10^{-4}

5.3. Effect of solid volume fraction

To better understand effects of solid volume fraction on heat flow phenomena, streamlines and isotherms for various solid volume fractions at Ha = 0.1 and Ra =10^4 are plotted in Fig 4. It is found that when the nanosolid volume fraction is increasingly higher, the circulation intensity significantly decreases. For the pure base fluid or pure water [φ = 0], there appears one strong circulation occupying an entire cavity whereas the flow circulation undergoes a transformation into two small weaker vortices at higher solid volume fraction. With regard to isotherms, adding solid nanoparticles to the base fluid clearly changes the isotherm pattern. In the case of pure base fluid, wavy isotherm lines manifest in the middle of cavity, attributed to vigorous fluid motion facilitating energy convection across the domain. In addition, the temperature gradients at the wall intensify particularly at the corners. Then the isotherms are converted from irregular shape due to a strong flow circulation for pure fluid case to essentially parallel lines with the presence of nanoparticles. As the solid volume fraction further increases, the pair of flow circulations gets even weaker. The viscos effect imposed by nanoparticles impedes the flow dynamics. Consequently, the diminished flow activity results in reduced heat transport across the cavity, establishing heat conduction as the predominant mode of heat transfer.

(a)   φ = 0.0

(b)   φ = 0.0001

(c)   φ = 0.0002

(d)   φ = 0.0003
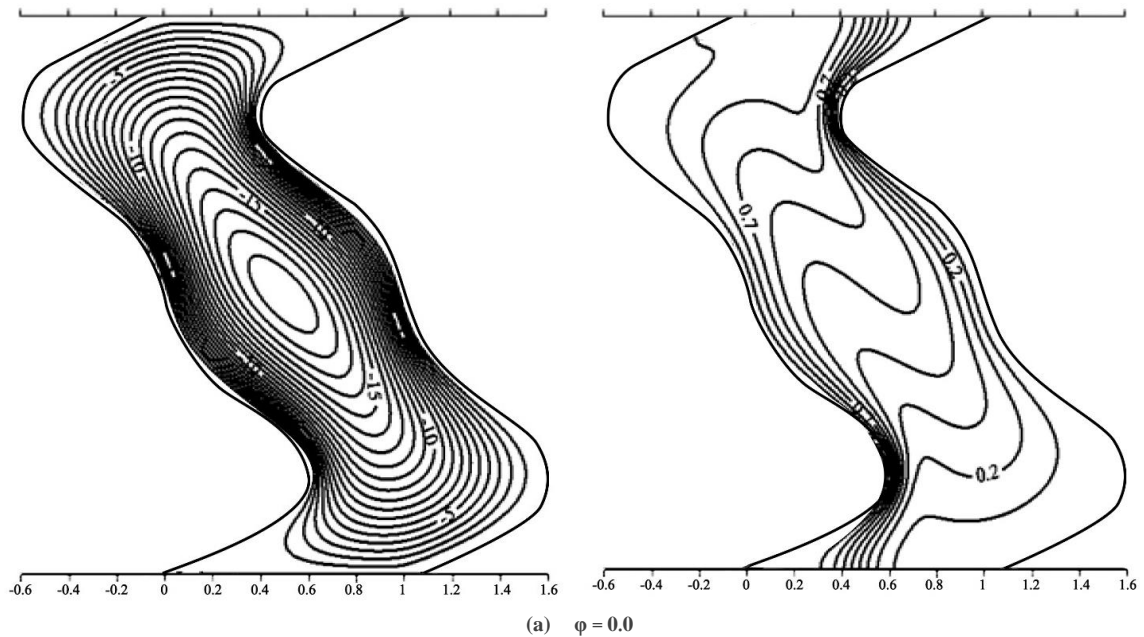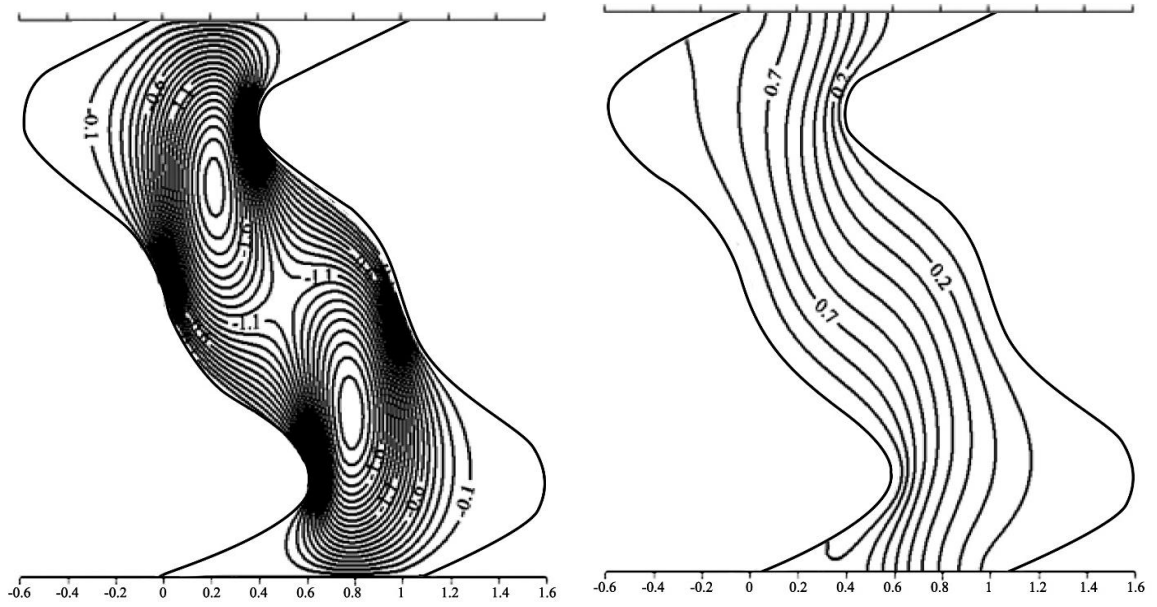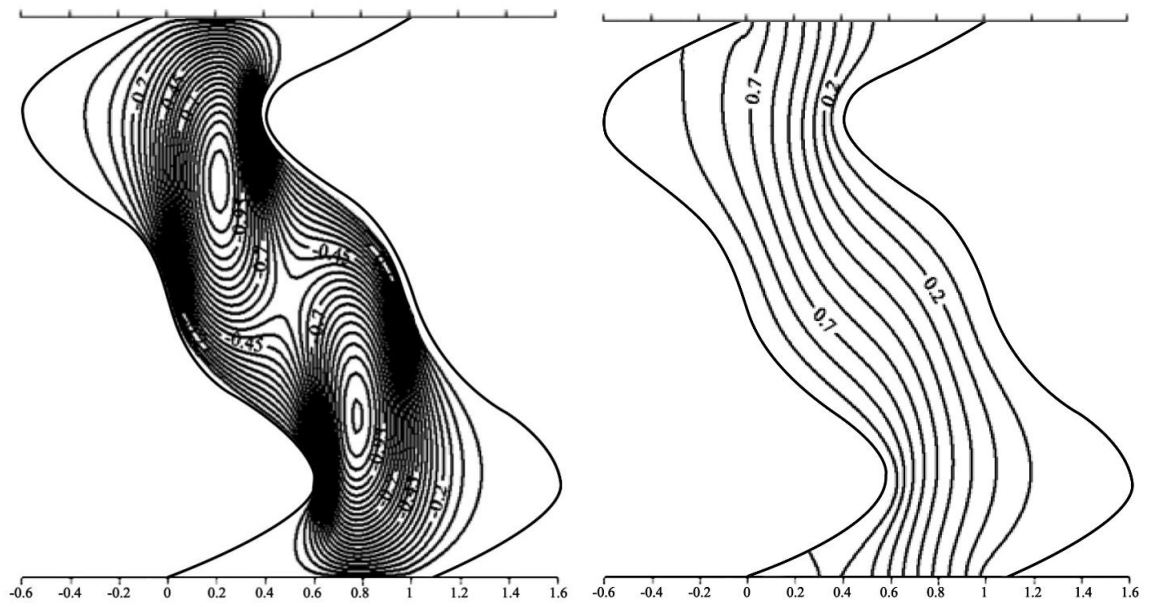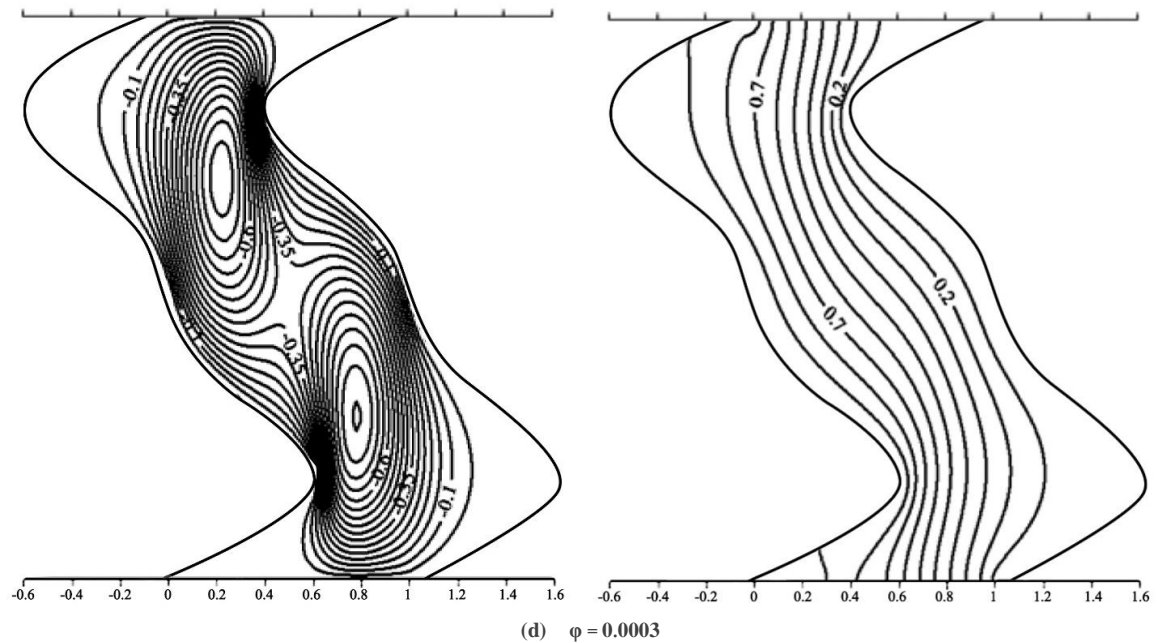
Fig 4: Streamlines (left) and isotherms (right) for various solid volume fraction at Ha = 0.1 and Ra = 10^4

5.4. Effect of wavy wall geometry parameters

Figure 5 presents streamlines (left) and isotherms (right) for various geometries of the zigzag wall surface at Ha = 0.5, φ = 0.0001 and Ra =10^5. The wall geometry parameters based on the sinusoidal function involve values of wave amplitude and the ratio of them. The results reveal that both the flow field and accordingly thermal field are significantly affected by the wave form of the wavy wall corresponding to sinusoidal functions of two components given in equation 13. It can be seen that for Case 1 and Case 3, there clearly appear two counterclockwise vortices. In Case 2 the shape of each wavy wall exhibits two waves corresponding to a high variation of shape profile. It is seen that essentially one vortex is formed but its shape is stretched and distorted leading to irregular shape pattern with large area of intense gradients. This is due to high variation of wavy shape at the boundaries. High gradients of the streamline directly perturb the temperature distribution observed in the right figure. This result suggests that heat convection between the nanofluid inside and the hot wavy wall is significantly enhanced. On the other hand, for Case 3 in which only the one component (equation 13) contributes to the wavy profile, the flow field is relatively less perturbed by the wavy boundaries that are plainer in overall since a pattern of wall shape profile of a single regular wave is relatively smooth. The isotherms change their shape from random and irregular distribution observed in Cases 1 and 2 to the approximately even distribution parallel to the sidewalls of the wavy cavity. The corresponding temperature gradients appear nearly uniform indicating that the heat transfer by the conduction prevails.

(a) Case 1: $\alpha_1 = 0.5$ and $R_\alpha = 0.2$

(b) Case 2: $\alpha_1 = 2.5$ and $R_\alpha = 0.188$

(c) Case 3: $\alpha_1 = 0.607$ and $R_\alpha = 0$
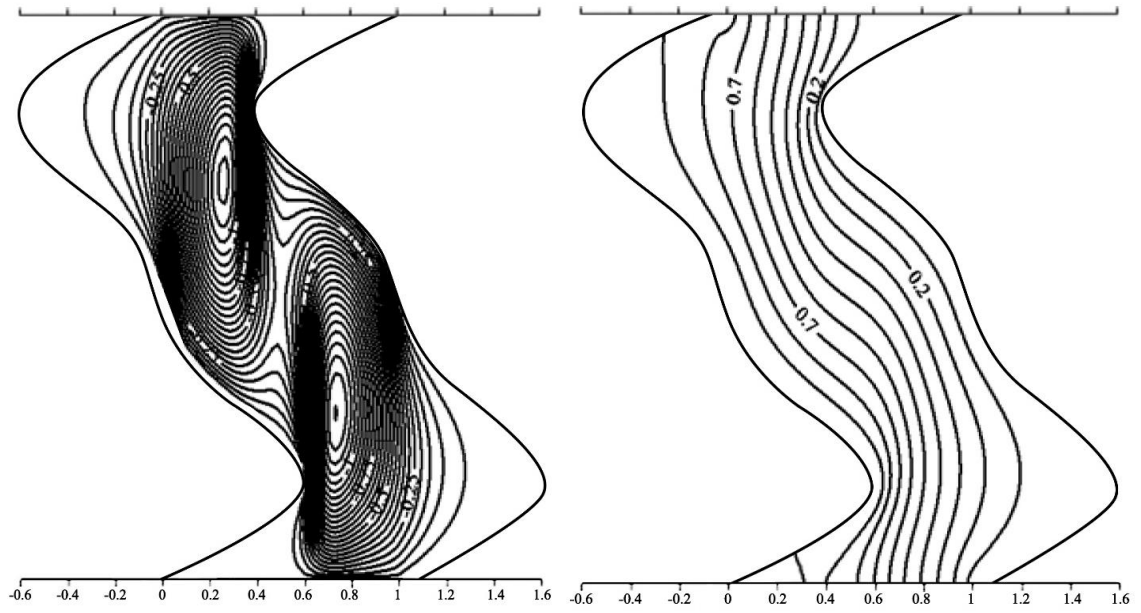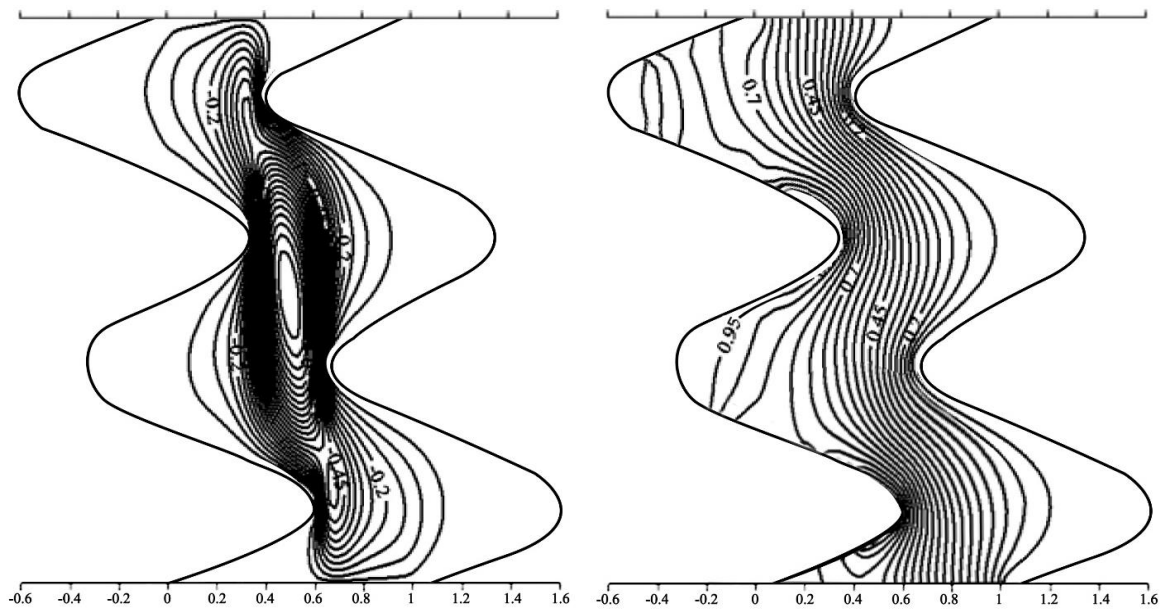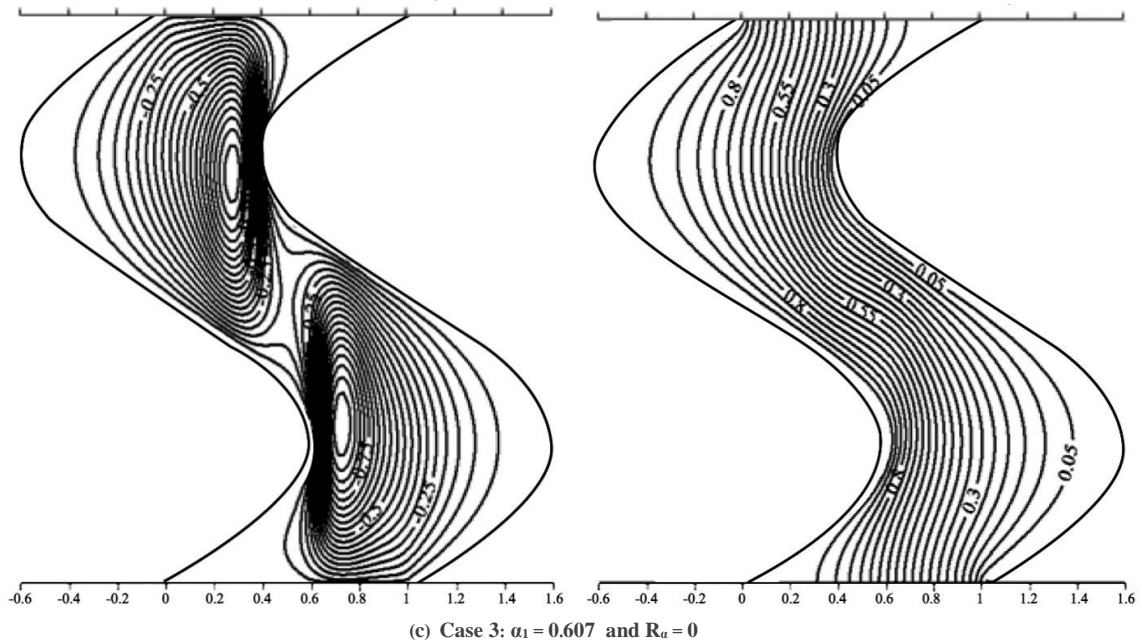
Fig 5: Streamlines (left) and isotherms (right) for variousamplitudes at Ha=0.5, $\varphi=10^{-4}$ and Ra =10^5

5.5. Mean Nusselt number results

In Fig 6, the relationship among the average Nusselt number, Rayleigh number, and volume fraction of nanoparticles is depicted for Case 3 ($\phi = 0.607$ and Ha = 0.1). The results reveal that with a solid volume fraction of $\phi = 0$ (pure water), the average Nusselt number (Nu_m) is very high. However, as the solid volume fraction increases, Nu_m decreases and reaches a minimum value at some intermediate solid volume fraction. Then it becomes independent of the Rayleigh number as the solid volume fraction gets larger. The Nu_m remains unchanged at volume fractions of 8×10^{-4}, 9×10^{-4} and 3.5×10^{-3} at Ra of 10^3, 10^4 and 10^5 respectively. This behavior can be explained by the growth of a thick thermal boundary layer, which increases with the volume fraction of nanoparticles. The nanofluid flow experiences significant suppression due to the high fraction of solid particles, leading to a higher effective viscosity. Consequently, there is a decrease in thermal energy transport through the fluid. Moreover, a substantial increase in the proportion of nanoparticles results in an enhancement of the nanofluid's effective thermal conductivity. As a consequence, heat transfer within the wavy cavity is primarily governed by conduction. These observations offer an additional rationale for the variation in the Nusselt number at higher solid volume fractions.

Figure 7 shows the change in the mean Nusselt number (Nu_m) with solid volume fraction at Ra = 10^5. Effects of different Ha are investigated for Case 3 [$\alpha_1 = 0.607$, $\alpha_2 = 0$ and $R_\alpha = 0$]. As seen in the result, the distribution of the mean Nusselt number depends significantly on the Hartmann (Ha). Without magnetic field [i.e., Ha = 0], Nu_m remains almost unchanged for the range of solid volume fractions considered. At greater Hartmann number, the Nu_m decreases significantly. This is because, the Lorentz force induced by magnetic field suppresses the flow strength causing convection mode of heat transfer to degrade. At higher Ha, convective effect is lessened. Once the convection and conduction become comparable or within the same order of magnitude, the effect of volume fraction becomes pronounced. As a result, when the volume fraction increases the Nu_m decreases since heat conduction contributes more with volume fraction. In this case, the retarding effect is shown to be larger than the driving force due to the buoyancy effect on flows therefore a significant reduction of the mean Nusselt number results. This indicates that the force induced by magnetic field is the dominant force that alters the flow behavior inside the wavy cavity. However, the Nu_m gets leveled off as heat conduction prevails at larger volume fractions of 6×10^{-5} and 1×10^{-4} at Ha of 0.6 and 0.3 respectively. Figure 8 displays how the average Nusselt number varies with solid volume fraction for different wave forms [(1) $\alpha_1 = 0.5$, $\alpha_2 = 0.1$ and $R_\alpha = 0.2$], [(2) $\alpha_1 = 2.5$, $\alpha_2 = 0.47$ and $R_\alpha = 0.188$] and [(3) $\alpha_1 = 0.607$, $\alpha_2 = 0$ and $R_\alpha = 0$] respectively. It is obvious that the distribution of the mean Nusselt number strongly depends on the wave form of the wavy wall whereas the change in solid volume fraction has much less effect on it. It indicates that the wave form of wavy is a dominant effect on the mean Nusselt number. It can be clearly seen that the in case 2the mean Nusselt number reaches 3.204 which is highest, while case 3 gives the lowest mean Nusselt number and reveals pure

conduction at volume fraction greater than 5×10^{-5}. Therefore, case 2 is considered to be the optimum wave form to enhance the heat convection. This finding is consistently supported by the result observed in Fig 5. The reason for this is that the presence of pronounced irregularities in the surface geometry which intensify a convective flow, thereby raising the Nu_m. Consequently, by systematically choosing the geometric parameters of the undulating wall, one can raise the heat transfer efficiency.
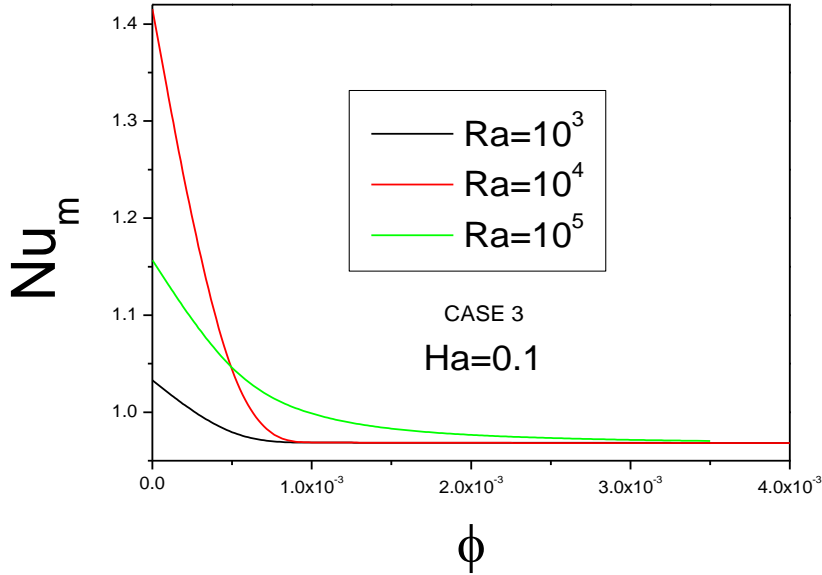
Fig 6: Variation of mean Nusselt number with Rayleigh number and solid volume fraction at Ha=0.1 and for Case 3 [α_1 = 0.607 and R_α = 0]
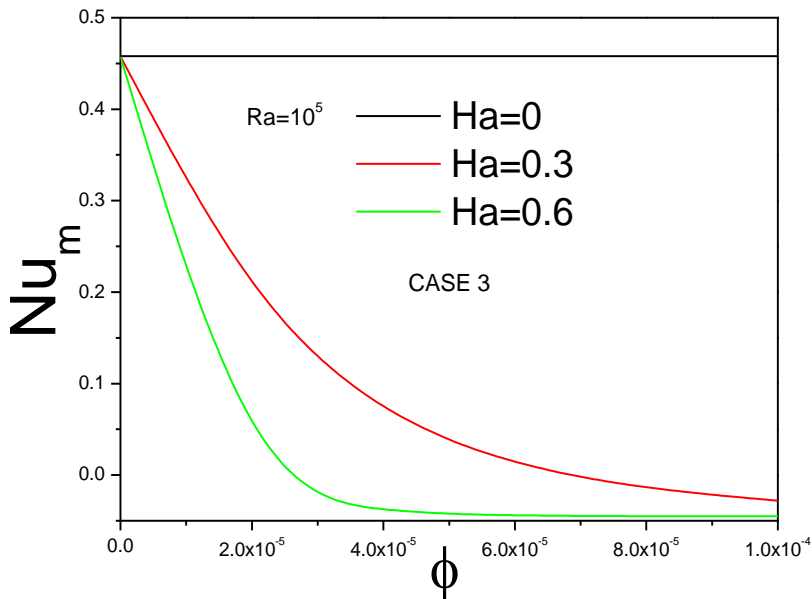
Fig 7: Variation of mean Nusselt number with Hartmann number and solid volume fraction at Ra = 10^5 and for Case 3 [α_1 = 0.607 and R_α = 0]
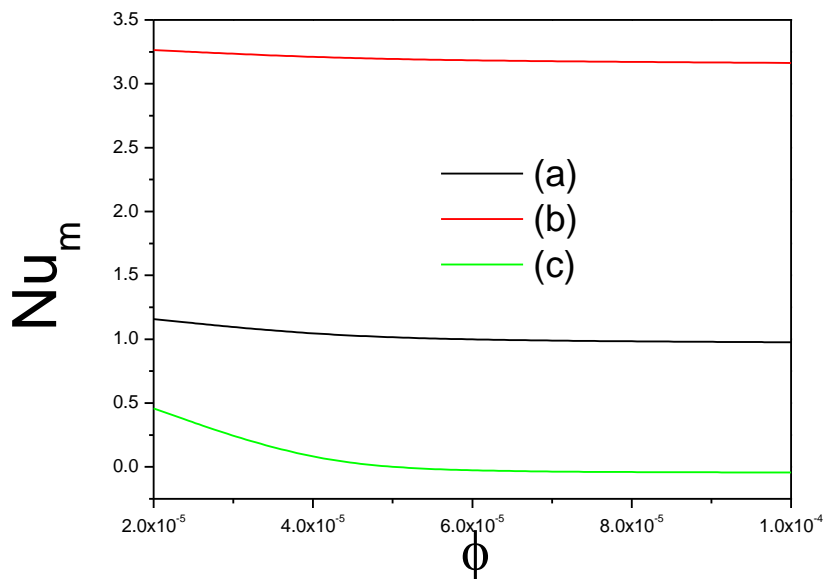
Fig 8: Variation of mean Nusselt number with solid volume fraction for various waveforms [(a) α_1 = 0.5 and R_α = 1/5], [(b) R_α = 0.47/2.5 and α_2 = 0.47] and [(c) α_1 = 0.607 and R_α = 0]

6. Conclusions

The study investigated the combined mixed convective heat flow behaviors of water-Al_2O_3 nanofluid within a wavy cavity subjected to a magnetic field. The wavy cavity's geometry was designed based on various wave functions. The primary findings from the analysis of the can be succinctly summarized as follows:

1. The intensity of flow circulation increases with a higher Rayleigh number (Ra), leading to distorted and curved isotherms, consequently enhancing convective heat transfer.
2. At high Hartmann number (Ha), the Lorentz force induced by the magnetic field becomes significant thereby weakening a flow circulation in the cavity. As a result, the convective effect is greatly decreased.
3. Flow circulation intensity diminishes with an increase in the volume percentage of solid particles.
4. High volume fraction of nanoparticles results in a thickened thermal boundary layer, accompanied by a reduced flow circulation rate due to the densely packed solid particles, causing an increased effective viscosity. Consequently, the mean Nusselt number (Nu_m) decreases with an increased volume fraction.
5. The Num value reaches minimum and remains nearly constant at a certain value of solid volume fraction. This certain value of volume fraction gets higher for higher Ra and lower Ha.
6. In case (b) [α_1=2.5 and R_α = 0.188], the wall shape composed of two full waves proves to be the most effective form in enhancing convective heat transfer at the mean Nusselt number of 3.204 with stream function of 1.638.

7. Acknowledgments

Reference

[1]   Z. Guo, A Review on Heat Transfer Enhancement with Nanofluids, *Journal of Enhanced Heat Transfer,* Vol. 27, No. 1, pp. 1-70, 2020, 2020.

[2]   M. Muthtamilselvan, P. Kandaswamy, J. Lee, Heat transfer enhancement of copper-water nanofluids in a lid-driven enclosure, *Communications in Nonlinear Science and Numerical Simulation,* Vol. 15, No. 6, pp. 1501-1510, 2010/06/01/, 2010.

[3]   F. Talebi, A. H. Mahmoudi, M. Shahi, Numerical study of mixed convection flows in a square lid-driven cavity utilizing nanofluid, *International Communications in Heat and Mass Transfer,* Vol. 37, No. 1, pp. 79-90, 2010/01/01/, 2010.

[4]   M. Shahi, A. H. Mahmoudi, F. Talebi, Numerical study of mixed convective cooling in a square cavity ventilated and partially heated from the below utilizing nanofluid, *International Communications in Heat and Mass Transfer,* Vol. 37, No. 2, pp. 201-213, 2010/02/01/, 2010.

[5]   M. Salari, M. M. Tabar, A. M. Tabar, H. A. Danesh, Mixed Convection of Nanofluid Flows in a Square Lid-Driven Cavity Heated Partially From Both the Bottom and Side Walls, *Numerical Heat Transfer, Part A: Applications,* Vol. 62, No. 2, pp. 158-177, 2012/07/15, 2012.

[6]   R. Nasrin, M. A. Alim, A. J. Chamkha, Modeling of mixed convective heat transfer utilizing nanofluid in a double lid-driven chamber with internal heat generation, *International Journal of Numerical Methods for Heat & Fluid Flow,* Vol. 24, No. 1, pp. 36-57, 2014.

[7]   M. A. Sheremet, I. Pop, Mixed convection in a lid-driven square cavity filled by a nanofluid: Buongiorno's mathematical model, *Applied Mathematics and Computation,* Vol. 266, pp. 792-808, 2015/09/01/, 2015.

[8]   A. I. Alsabery, M. A. Ismael, A. J. Chamkha, I. Hashim, Mixed convection of Al2O3-water nanofluid in a double lid-driven square cavity with a solid inner insert using Buongiorno's two-phase model, *International Journal of Heat and Mass Transfer,* Vol. 119, pp. 939-961, 2018/04/01/, 2018.

[9]   E. Abu-Nada, A. J. Chamkha, Mixed convection flow of a nanofluid in a lid-driven cavity with a wavy wall, *International Communications in Heat and Mass Transfer,* Vol. 57, pp. 36-47, 2014/10/01/, 2014.

[10]   M. Jafari, M. Farhadi, K. Sedighi, E. Fattah, Effect of Wavy Wall on Convection Heat Transfer of Water-Al2O3Nanofluid in a Lid-Driven Cavity Using Lattice Boltzmann Method, *International Journal of Engineering Transactions A: Basics,* Vol. 25, No. 2, pp. 165-175, 2012.

[11]   C. C. Cho, C. L. Chen, C. K. Chen, Mixed convection heat transfer performance of water-based nanofluids in lid-driven cavity with wavy surfaces, *International Journal of Thermal Sciences,* Vol. 68, pp. 181-190, 2013/06/01/, 2013.

[12]   M. Mamourian, K. Milani Shirvan, R. Ellahi, A. B. Rahimi, Optimization of mixed convection heat transfer with entropy generation in a wavy surface square lid-driven cavity by means of Taguchi approach, *International Journal of Heat and Mass Transfer,* Vol. 102, pp. 544-554, 2016/11/01/, 2016.

[13]   C. C. Cho, Heat transfer and entropy generation of mixed convection flow in Cu-water nanofluid-filled lid-driven cavity with wavy surface, *International Journal of Heat and Mass Transfer,* Vol. 119, pp. 163-174, 2018/04/01/, 2018.

[14]   A. I. Alsabery, M. A. Ismael, A. J. Chamkha, I. Hashim, Numerical Investigation of Mixed Convection and Entropy Generation in a Wavy-Walled Cavity Filled with Nanofluid and Involving a Rotating Cylinder, *Entropy,* Vol. 20, No. 9, pp. 664, 2018.

[15]   A. I. Alsabery, M. A. Sheremet, A. J. Chamkha, I. Hashim, Impact of nonhomogeneous nanofluid model on transient mixed convection in a double lid-driven wavy cavity involving solid circular cylinder, *International Journal of Mechanical Sciences,* Vol. 150, pp. 637-655, 2019/01/01/, 2019.

[16]   F. M. Azizul, A. I. Alsabery, I. Hashim, Heatlines visualisation of mixed convection flow in a wavy heated cavity filled with nanofluids and having an inner solid block, *International Journal of Mechanical Sciences,* Vol. 175, pp. 105529, 2020/06/01/, 2020.

[17]   K. Hosseinzadeh, S. Akbari, S. Faghiri, M. B. Shafii, Optimization approach for MoS2-water ethylene glycol mixture nanofluid flow in a wavy enclosure, *International Journal of Thermofluids,* Vol. 18, pp. 100337, 2023/05/01/, 2023.

[18]   K. Hosseinzadeh, E. Montazer, M. B. Shafii, D. D. Ganji, Heat transfer hybrid nanofluid (1-Butanol/MoS–FeO) through a wavy porous cavity and its optimization, *International Journal of Numerical Methods for Heat & Fluid Flow,* Vol. 31, No. 5, pp. 1547-1567, 2021.

[19]   N. Alipour, B. Jafari, K. Hosseinzadeh, Optimization of wavy trapezoidal porous cavity containing mixture hybrid nanofluid (water/ethylene glycol Go–Al2O3) by response surface method, *Scientific Reports,* Vol. 13, No. 1, pp. 1635, 2023/01/30, 2023.

[20]   P. Pattanavanitkul, W. Pakdee, Parametric Study of Unsteady Flow and Heat Transfer of Compressible Helium–Xenon Binary Gas through a Porous Channel Subjected to a Magnetic Field, *Fluids,* Vol. 6, No. 11, pp. 392, 2021.

[21]   H. F. Oztop, K. Al-Salem, I. Pop, MHD mixed convection in a lid-driven cavity with corner heater, *International Journal of Heat and Mass Transfer,* Vol. 54, No. 15, pp. 3494-3504, 2011/07/01/, 2011.

[22]   F. Selimefendigil, H. F. Öztop, Numerical study of MHD mixed convection in a nanofluid filled lid driven square enclosure with a rotating cylinder, *International Journal of Heat and Mass Transfer,* Vol. 78, pp. 741-754, 2014/11/01/, 2014.

[23]   S. Hussain, K. Mehmood, M. Sagheer, MHD mixed convection and entropy generation of water–alumina nanofluid flow in a double lid driven cavity with discrete heating, *Journal of Magnetism and Magnetic Materials,* Vol. 419, pp. 140-155, 2016/12/01/, 2016.

[24]   M. Sheikholeslami, A. J. Chamkha, Flow and convective heat transfer of a ferro-nanofluid in a double-sided lid-driven cavity with a wavy wall in the presence of a variable magnetic field, *Numerical Heat Transfer, Part A: Applications,* Vol. 69, No. 10, pp. 1186-1200, 2016/05/18, 2016.

[25]   H. F. Öztop, A. Sakhrieh, E. Abu-Nada, K. Al-Salem, Mixed convection of MHD flow in nanofluid filled and partially heated wavy walled lid-driven enclosure, *International Communications in Heat and Mass Transfer,* Vol. 86, pp. 42-51, 2017/08/01/, 2017.

[26]   S. Hussain, H. F. Öztop, K. Mehmood, N. Abu-Hamdeh, Effects of inclined magnetic field on mixed convection in a nanofluid filled double lid-driven cavity with volumetric heat generation or absorption using finite element method, *Chinese Journal of Physics,* Vol. 56, No. 2, pp. 484-501, 2018/04/01/, 2018.

[27]   A. I. Alsabery, M. A. Sheremet, M. Sheikholeslami, A. J. Chamkha, I. Hashim, Magnetohydrodynamics energy transport inside a double lid-driven wavy-walled chamber: Impacts of inner solid cylinder and two-phase nanoliquid approach, *International Journal of Mechanical Sciences,* Vol. 184, pp. 105846, 2020/10/15/, 2020.

[28]   H. K. Hamzah, F. H. Ali, M. Hatami, MHD mixed convection and entropy generation of CNT-water nanofluid in a wavy lid-driven porous enclosure at different boundary conditions, *Scientific Reports,* Vol. 12, No. 1, pp. 2881, 2022/02/21, 2022.

[29]   K. Hosseinzadeh, M. A. Erfani Moghaddam, S. Nateghi, M. Behshad Shafii, D. D. Ganji, Radiation and convection heat transfer optimization with MHD analysis of a hybrid nanofluid within a wavy porous enclosure, *Journal of Magnetism and Magnetic Materials,* Vol. 566, pp. 170328, 2023/01/15/, 2023.

[30]   N. Alipour, B. Jafari, K. Hosseinzadeh, Thermal analysis and optimization approach for ternary nanofluid flow in a novel porous cavity by considering nanoparticle shape factor, *Heliyon,* Vol. 9, No. 12, pp. e22257, 2023/12/01/, 2023.

[31]   K. Hosseinzadeh, S. Roghani, A. R. Mogharrebi, A. Asadi, D. D. Ganji, Optimization of hybrid nanoparticles with mixture fluid flow in an octagonal porous medium by effect of radiation and magnetic field, *Journal of Thermal Analysis and Calorimetry,* Vol. 143, No. 2, pp. 1413-1424, 2021/01/01, 2021.

[32]   K. Hosseinzadeh, M. Roshani, M. A. Attar, D. D. Ganji, M. B. Shafii, Heat transfer study and optimization of nanofluid triangular cavity with a pentagonal barrier by finite element approach and RSM, *Heliyon,* Vol. 9, No. 9, pp. e20193, 2023/09/01/, 2023.

[33]   A. K. Rostami, K. Hosseinzadeh, D. D. Ganji, Hydrothermal analysis of ethylene glycol nanofluid in a porous enclosure with complex snowflake shaped inner wall, *Waves in Random and Complex Media,* Vol. 32, No. 1, pp. 1-18, 2022/01/02, 2022.

[34]   H. J. Kim, S.-H. Lee, J.-H. Lee, S. P. Jang, Effect of particle shape on suspension stability and thermal conductivities of water-based bohemite alumina nanofluids, *Energy,* Vol. 90, pp. 1290-1297, 2015/10/01/, 2015.

[35]   M. Kong, S. Lee, Performance evaluation of Al2O3 nanofluid as an enhanced heat transfer fluid, *Advances in Mechanical Engineering,* Vol. 12, No. 8, pp. 1687814020952277, 2020/08/01, 2014.

[36]   M. Sheikholeslami, M. Gorji-Bandpy, D. D. Ganji, Numerical investigation of MHD effects on Al2O3–water nanofluid flow and heat transfer in a semi-annulus enclosure using LBM, *Energy,* Vol. 60, pp. 501-510, 2013/10/01/, 2013.

[37]   C.-C. Cho, C.-L. Chen, C. o.-K. Chen, Natural convection heat transfer performance in complex-wavy-wall enclosed cavity filled with nanofluid, *International Journal of Thermal Sciences,* Vol. 60, pp. 255-263, 2012/10/01/, 2012.

[38]   T. Mahalakshmi, N. Nithyadevi, H. F. Oztop, N. Abu-Hamdeh, Natural convective heat transfer of Ag-water nanofluid flow inside enclosure with center heater and bottom heat source, *Chinese Journal of Physics,* Vol. 56, No. 4, pp. 1497-1507, 2018/08/01/, 2018.

[39]   M. A. Mansour, M. A. Y. Bakier, Free convection heat transfer in complex-wavy-wall enclosed cavity filled with nanofluid, *International Communications in Heat and Mass Transfer,* Vol. 44, pp. 108-115, 2013/05/01/, 2013.

[40]   A. Mansour, A. Chamkha, R. Mohamed, M. Aziz, S. Ahmed, MHD natural convection in an inclined cavity filled with a fluid saturated porous medium with heat source in the solid phase, *Nonlinear Analysis. Modelling and Control,* Vol. 1, 03/04, 2010.

[41]   T. Grosan, C. Revnic, I. Pop, D. B. Ingham, Magnetic field and internal heat generation effects on the free convection in a rectangular cavity filled with a porous medium, *International Journal of Heat and Mass Transfer,* Vol. 52, No. 5, pp. 1525-1533, 2009/02/01/, 2009.

[42]   B. V. R. Kumar, P. V. S. N. Murthy, P. Singh, Free convection heat transfer from an isothermal wavy surface in a porous enclosure, *International Journal for Numerical Methods in Fluids,* Vol. 28, No. 4, pp. 633-661, 1998.

[43]   M. Haajizadeh, A. F. Ozguc, C. L. Tien, Natural convection in a vertical porous enclosure with internal heat generation, *International Journal of Heat and Mass Transfer,* Vol. 27, No. 10, pp. 1893-1902, 1984/10/01/, 1984.